PROBING THE INNERMOST REGIONS OF PROTOSTELLAR OUTFLOWS WITH THE SUBMILLIMETER ARRAY.

N. Hirano, C.-F. Lee, S.-Y. Liu, H. Shang, *Academia Sinica, Institute of Astronomy and Astrophysics, Taipei, Taiwan, (hirano@asiaa.sinica.edu.tw).*

It is known that several highly collimated molecular outflows driven by deeply embedded young stellar objects are associated with extremely high-velocity (EHV) emission component running along the axes of the lobes (e.g. Bachiller, 1986). Since the EHV molecular outflows having terminal velocities of 50–150 km s^{-1} have large momenta comparable to those of the slowly moving (20–30 km s^{-1}) "classical" outflows, they are considered to be closely connected to the "primary jet" responsible for driving the broader molecular outflows. The EHV molecular outflows have been exclusively observed in the CO and SiO lines. Here we present the (sub) arcsecond SiO J=5–4 and 8–7, and CO J=3–2 images of three archetypical outflows with EHV components, i.e. HH211, HH212, and L1448, observed with the Submillimeter Array (SMA)[1] .

The HH211 outflow in the IC 348 molecular cloud complex (D∼315 pc) is driven by a low-luminosity (3.6 $L_{\odot}$) Class 0 protostar. This outflow is considered to be extremely young, with a dynamical age of only ∼750 yr. The high-resolution (1.5″) CO J=2–1 observations by Gueth & Guilloteau (1999) revealed a remarkable structure: the low-velocity CO delineates a pair of shells whose tips are associated with NIR H_2 emission, while the high-velocity CO traces a narrower feature whose velocity increases linearly with distance from the star.

Bisecting the CO lobe is a narrow jet of thermal SiO emission, which is considered to trace the dense shocked gas. High resolution (1-2″) observations of SiO J=8–7 (Palau et al. 2006; Lee et al. 2007b), 5–4 (Hirano et al. 2006), and 3–2 (Hirano et al. 2007) have been done using the SMA and the Nobeyama Millimeter Array. As shown in Fig.1, the SiO jet is resolved into a chain of knots separated by 4″ (∼1000 AU). The SiO knots have their H_2 counterparts except the ones in close vicinity of the central source where the extinction is large. The knotty structure is more prominent in the higher SiO transition. The innermost knots located at ±2″ from the source are prominent in the J=8–7 and 5–4 maps, while barely seen in the J=1–0 map. Hirano et al. (2006) estimated that these knots have a temperature >300-500 K and density (0.5-1) × 10^7 cm^{-3}. These densities and temperatures are much higher than those inferred for the CO shell component, indicating that the SiO jet has a different origin. The most likely possibility is that the SiO jet traces the densest part of the primary wind. This identification is strengthened by the PV diagrams of SiO J=8–7 and 5–4 emission, which show a large (projected) velocity dispersion (∼30 km s^{-1}) close to the star. This velocity feature, absent from the CO emission, is reminiscent of that predicted in the X-wind theory for optical forbidden lines (Shang et al. 1998). It may be indicative of a (perhaps unsteady) wide-angle wind that is stratified in density, as envisioned in our unified model of molecular outflows (Shang et al. 2006).

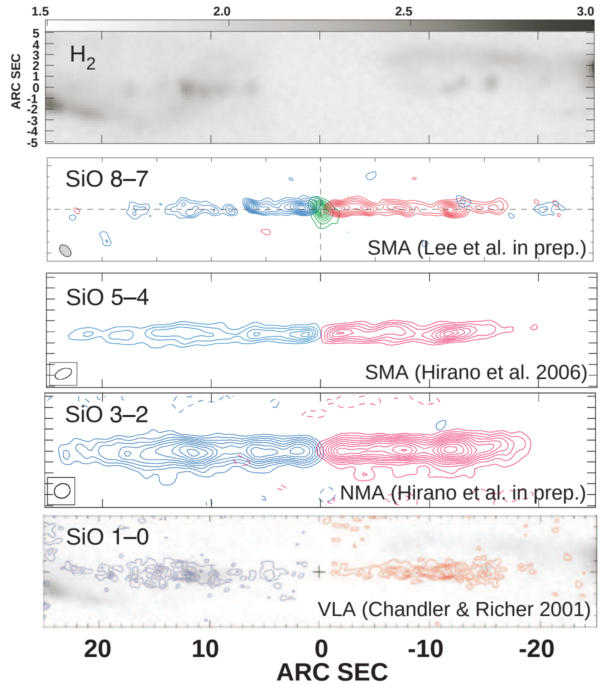

Figure 1: The infrared H_2 image (top) and the integrated blue and redshifted maps of the SiO J=8–7, J=5-4, 3-2, and 1-0 of teh HH211 outflow. All the images are rotated by −26° to align the major axis with the horizontal. The SiO J=1-0 map is from Chandler & Richer (2001)

The HH212 jet in the L1620 cloud of Orion (D∼460) pc is a remarkable jet with a length of ∼240″ (∼0.6 pc) powered by a low-luminosity (∼14 $L_{\odot}$) class 0 source, IRAS 05413-0104. It is highly collimated and highly symmetric with matched pairs of bow shocks on either side of the source (Zinneker et al. 1998; McCaughrean et al. 2002). The axis of this jet is believed to line within 5° of the plane of the sky; therefore, this jet is suitable for studying the dense and warm component in the close vicinity of its driving source.

Fig. 2 shows the SiO J=8–7 and CO 3–2 image observed with the SMA at an angular resolution of 1.16″×0.84″ (Lee et al. 2007a). The SiO emission is detected mainly along the jet axis. As in the case of HH211, the SiO jet consists of a chain of knots having a semiperiodic spacing of ∼3″ (∼1400 AU); each of the SiO knot has its H_2 counterpart. The innermost knot pair labeled SN and SS is located at ∼ ±1″ from the source. The CO 3–2 emission at high velocity is seen mainly

[1]The Submillimeter Array (SMA) is a joint project between the Smithsonian Astrophysical Observatory and the Academia Sinica Institute of Astronomy and Astrophysics, and is funded by the Smithsonian Institution and the Academia Sinica.

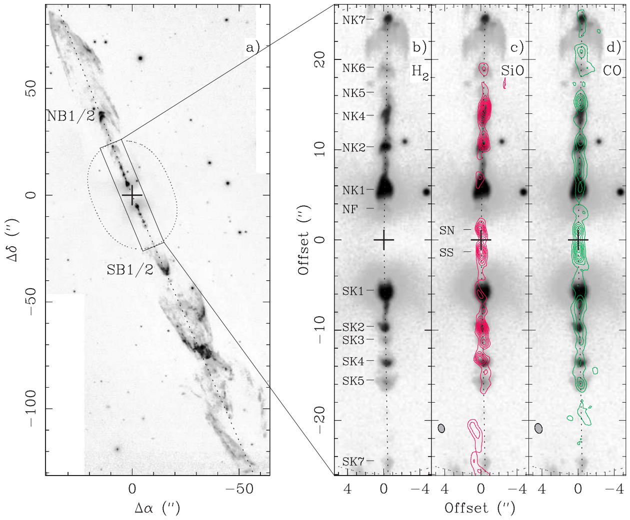

Figure 2: a) The H_2 image of the HH212 outflow from McCaughrean et al. (2002). b) The H_2 image rotated by 22.5° clockwise. (c) SiO emisison integrated from -21.1 to 16.0 km s^{-1}. (d) High velocity CO integrated from -18.4 to 7.1 and from 3.4 to 13.3 km s^{-1}. (Lee et al. 2007a)

along the jet axis and shows similar structure as the SiO jet. In the case of the HH212 jet, the CO emission is also detected at the innermost knot pair, SN and SS. This it different from the HH211 jet, toward which the innermost knot pair is barely seen in the CO 3–2 map. The low-velocity CO 3–2 delineates limb-brighened shells. These shells have a velocity structure that increases with the distance from the source on both redshifted and blueshifted sides, indicating that the shells are expanding mainly transversely perpendicular to the jet axis. Toward the bow shocks, the SiO emissioin is seen with a broad velocity range of $\sim$15 km s^{-1}. In the case of the HH212 jet, there is no systematic velocity difference between SiO and CO, although the velocity dispersion observed in CO tends to be smaller than that observed in SiO. Toward the innermost knots SN and SS, both SiO and CO are seen with a broad range of velocities, but with a lower mean velocity than that seen toward the bow shocks further away.

The EHV outflow powered by the class 0 source L1448-mm ($L\sim10L_\odot$, also called L1448C) consists of discrete condensations moving with radial velocities up to 70 km s^{-1} (Bachiller et al. 1990). Guilloteau et al. (1992) and Girart & Acord (2001) mapped the SiO J=2–1 emission from the EHV condensations close to the mm source with 2″ resolution and found two pairs of clumps (BI, BII, RI, and RII) separated by $\sim$4″. These four SiO J=2–1 clumps are located along the axis of the V-shaped cavities (P.A. $\sim$21°) with lower velocity traced by the interferometric CO J=1–0 map (Bachiller et al. 1995).

The SiO J=5–4 from the L1448-mm outflow was mapped with the SMA at an angular resolution of 1.26″×1.16″. Our SiO J=5–4 map show that the innermost pair of knots BI and RI in the SiO J=2–1 map is resolved into two or three knots. In the SiO J=5–4, the blueshifted emission is weaker than the redshifted one. In addition, the extent of the blueshifted SiO J=5–4 is obviously shorter than that of the SiO J=2–1 counterpart. The SiO J=5–4 emission mainly comes from the regions that corresponds to the innermost knot pair BI and RI, and barely seen in the position of BII that is located at $\sim$10″ (=3000 AU) from the star. This is not due to the effect of the primary beam attenuation because the field of view of the SMA at 217 GHz is 54″, which is large enough to cover the outer pair. Since the gas kinetic temperature of the L1448-mm outflow derived from the single-dish SiO observations is high enough (>700 K; Nisini et al. 2007) , the SiO J=5-4 is weak at BII probably because the density there is not high enough to excite the SiO molecule to the J=5 level. The dynamical age of the L1448-mm outflow was estimated to be $\sim$3500 yr (Bachiller et al. 1990). This suggests that the outflow driven by L1448-mm is more evolved stage as compared to the HH211 outflow with a dynamical age of $\sim$750 yr. It is possible that the SiO jet in the L1448-mm outflow in the later evolutionary stage has lower density than that in the HH211 outflow.

References

Bachiller, R. 1996, ARAA, 34, 111
Bachiller, R., Cernicharo, J., Martín-Pintado, J., Tafalla, M. & Lazareff, B. 1990, A&A, 231, 174
Bachiller, R., Guilloteau, S., Dutrey, A., Planesas, P., & Martín-Pintado, J. 1995, A&A, 299, 857
Chandler, C. J. & Richer, J. S. 2001, ApJ, 555, 139
Girart, J.M. & Acord, J.M.P. 2001, ApJ, 552, L63
Gueth, F. & Guilloteau, S. 1999, A&A, 343, 571
Guilloteau, S., Bachiller, R., Fuente, A., & Lucas, R. 1992, A&A, 265, L49
Hirano, N., Liu, S.-Y., Shang, H., Ho, P.T.P., Huang, H.-C., Kuan, Y.-J., McCaughrean, M.J. & Zhang, Q. ApJ, 636, L141
Hirano, N. et al. in preparation
Lee, C.-F., Ho, P.T.P., Beuther, H., Bourke, T.L., Hirano, N., Shang, H., & Zhang, Q. 2007a, ApJ, ApJ, 659, 499
Lee, C-F. et al. 2007b, in preparation
McCaughrean, M., Zinnecker, H., Andersen, M., Meeus, G., & Lodieu, N. 2002, The Messenger, 109, 28
Nisini, B., Codella, C., Giannini, T., Santiago Garcia, J., Richer, J.S., Bachiller, R., & Tafalla, M. 2007, A&A, 462, 163
Palau, A., Ho, P.T.P., Zhang, Q., Estalella, R., Hirano, N., Shang, H., Lee, C.-F., Bourke, T.L. Beuther, H., & Kuan, Y.-J. 2006, ApJ, 636, L137
Shang, H., Shu, F.H., & Glassgold , A.E. 1998, ApJ, 493, L91
Shang, H., Allen, A., Li, Z.-Y., Liu, C.-F., Chou, M.-Y., & Anderson, J. 2006, ApJ, 649, 845